



Research Article

## Mitigation of Enteric Methane Emission from Ruminant by Bioactive Compounds of *Rhodomyrtus tomentosa*: *In Silico* and *In Vitro* Studies

Sigit Puspito

Department of Animal Nutrition and Feed Science, Faculty of Animal Science, Universitas Gadjah Mada, Yogyakarta, Indonesia

Research Center for Animal Husbandry, National Research and Innovation Agency, Bogor, Indonesia

Asih Kurniawati\*, Hafi Luthfi Sanjaya, Muhlisin Muhlisin, Muhsin Al Anas and Bambang Suwignyo

Department of Animal Nutrition and Feed Science, Faculty of Animal Science, Universitas Gadjah Mada, Yogyakarta, Indonesia

Yenny Nur Anggraeny, Setiasih Setiasih, Wardi Wardi and Slamet Widodo

Research Center for Animal Husbandry, National Research and Innovation Agency, Bogor, Indonesia

Bambang Haryanto

Research Center for Sustainable Industrial and Manufacturing Systems, National Research and Innovation Agency, Banten, Indonesia

Noor Hudhia Krishna

Directorate of Laboratory Management, Research Facilities, and Science and Technology, National Research and Innovation Agency, Jakarta, Indonesia

Fernando Berton Zanchi

Bioinformatics and Medicinal Chemistry Laboratory, Oswaldo Cruz Foundation Rondônia (LABIOQUIM-Fiocruz-RO), Porto Velho, Rondônia, Brazil

\* Corresponding author. E-mail: asihkurniawati@ugm.ac.id

DOI: 10.14416/j.asep.2025.12.005

Received: 16 July 2025; Revised: 4 September 2025; Accepted: 30 October 2025; Published online: 22 December 2025

© 2025 King Mongkut's University of Technology North Bangkok. All Rights Reserved.

### Abstract

The livestock sector significantly contributes to greenhouse gas emissions, primarily methane (CH<sub>4</sub>) from enteric fermentation in ruminants. Methanogenesis in ruminants is facilitated by hydrogenotrophic methanogens and the key enzyme, namely Methyl Coenzyme Reductase (MCR). This study explores the potential of bioactive compounds derived from *Rhodomyrtus tomentosa* as MCR enzyme inhibitors to mitigate methane emissions. Twelve bioactive compounds were selected for *in silico* molecular docking against the MCR enzyme. Docking results indicated Rhodomyrtone, Tomentodione E, and Myricetin had the highest binding affinities with binding affinities of -9.5, -8.7, and -8.3 kcal/mol, respectively, outperforming the natural substrate *Coenzyme B*. ADMET predictions confirmed the drug-likeness and safety profiles of these compounds. Rhodomyrtone was further subjected to molecular dynamics (MD) simulations, demonstrating stable interactions with MCR, indicated by consistent RMSD, RMSF, and Rg values. An *in vitro* gas production technique evaluated Rhodomyrtone's efficacy in reducing methane emissions, using doses of 0.125 and 0.25 µg/ml. Results showed a non-significant reduction of 10% in methane production, suggesting the need for optimized dosing. This study highlights rhodomyrtone as a promising anti-methanogen agent, with potential implications for reducing methane emissions from ruminants. Future research should focus on dose optimization and the exploration of synergistic effects with other anti-methanogenic compounds to maximize methane reduction.

**Keywords:** Livestock emission, Methane mitigation, Methyl-coenzyme M reductase, Molecular docking, *Rhodomyrtus tomentosa*

## 1 Introduction

In addition to being a sector affected by climate change, the livestock sector is also a sector that contributes to greenhouse gas emissions from its production activities. According to FAO [1], total emissions from global livestock amounted to 7.1 Gigatons carbon dioxide (CO<sub>2</sub>)-eq per year. The emissions in the form of methane (CH<sub>4</sub>), nitrous oxide (N<sub>2</sub>O), and carbon dioxide reach 44%, 29%, and 27%, respectively [2], [3]. The livestock sector in Indonesia emits greenhouse gases of 31,828 Gg CO<sub>2</sub> Eq. or 30% of the agricultural sector emissions, of which 55.4% is from enteric rumen fermentation, which mainly produces methane, according to the Ministry of Environment and Forestry [4].

Methane gas is a direct emission from the livestock sector, especially from ruminants. The adverse effects of the process are loss of energy for productivity and methane emissions to the environment [5], [6]. Livestock, especially large ruminants, and their supply chains, contribute significantly to anthropogenic emissions of the potent greenhouse gases (GHGs) methane and nitrous oxide [7]. Ruminants, especially adult cattle, can emit 80–110 Kg/year of methane gas.

Methane in ruminants is mainly produced by a hydrogenotrophic methanogen that converts CO<sub>2</sub> and H<sub>2</sub> into methane through the methanogenesis pathway. Hydrogenotrophic is the dominant methanogen in the rumen [8]. The methanogenesis pathway requires a key enzyme in methane formation, namely Methyl Coenzyme Reductase (MCR). An important function of the enzyme methyl-CoM reductase is as a catalyst of the last stage of methanogenesis to reduce methyl-S-CoM to methane with coenzyme B as an electron donor and coenzyme F430 as a prosthetic group [9]–[11].

Several strategies have been carried out in the past few decades to mitigate methane emissions from ruminants. One of them is the application of an anti-methanogen or inhibitor for the MCR enzyme. The use of tropical plants with compounds possessing anti-methanogen activity began to be widely researched as an antibiotic alternative since it has been banned as a growth promoter in animal production. Antibiotic administration as a ruminant feed additive has proven to reduce methane production in ruminants [12], [13].

With its high plant biodiversity in Indonesia, many medicinal plants with antimicrobial compounds can potentially be applied as anti-methanogenic, one of which is *Keramunting* (*Rhodomyrtus tomentosa*).

This plant is widely used as a medicine for diseases related to bacterial and viral infections, such as gastritis, hepatitis, diarrhea, abscesses, and bleeding [14], [15]. Several studies showed the potential of phytochemical content in *R. tomentosa* leaves as an antimicrobial agent [16]–[21]. Due to the antimicrobial activity [22], compounds in *R. tomentosa* have potential as anti-methanogens for methane mitigation efforts. Regarding the research efficiency, before wet laboratory work was conducted, a tool was needed as an initial screening tool that saves time and resources, and can test all these compounds. *In silico* studies, such as molecular docking, can be the right tool to test all these compounds against the MCR enzyme. Molecular docking can be a quick tool for initial screening by looking at the binding strength between the compounds and the MCR enzyme. Molecular docking data present the interaction between compounds and their protein targets, which can be essential for developing new antimicrobial compounds with anti-methanogenesis activity [23]. Based on the molecular docking data, a wet laboratory study using *in vitro* rumen fermentation methods can be conducted further to study reducing methane production for the most promising phytochemical compounds in *R. tomentosa*.

## 2 Materials and Methods

### 2.1 *In silico* study

#### 2.2.1 Ligand and protein target preparation



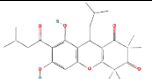
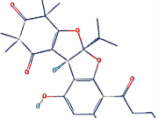
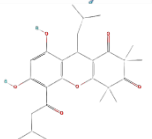
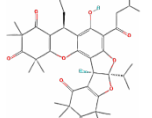

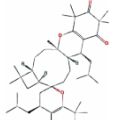
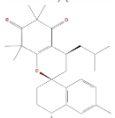
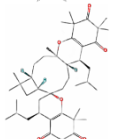
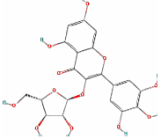
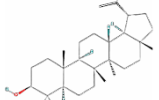
**Figure 1:** Protein Target MCR (methyl-CoM reductase) consists of 2 subunits: alpha subunits with chains A and D and beta subunits with chains B and E.

Twelve bioactive compounds from *R. tomentosa* were selected as ligands (Table 1). Ligands were prepared using ChimeraX 1.16. MCR target protein (Figure 1)

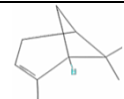

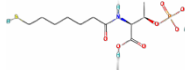
was obtained from Protein Data Bank (RCSB PDB - 7XSM <http://doi.org/10.2210/pdb7xsm/pdb>). The MCR target protein was prepared with AutoDockTools

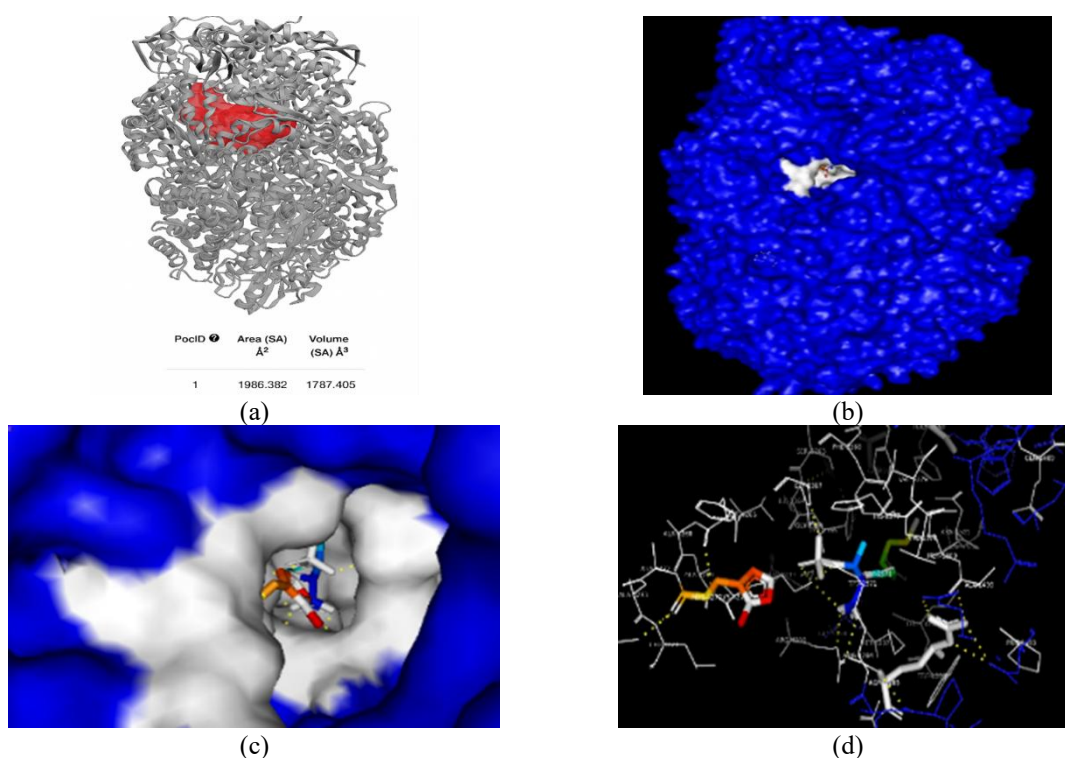
version 1.5.7, and the docking process was performed with AutoDock Vina in PyRx v0.8 software.

**Table 1:** Bioactive compound of *R. tomentosa* as ligand of molecular docking process.

No	Ligand	Classification	Formulas	Pubchem ID	2D Structure	Ref
1	Rhodomyrtone	Phenolic	C <sub>26</sub> H <sub>34</sub> O <sub>6</sub>	44237956		[16], [24]
2	Rhodomyrtosone A	Phenolic	C <sub>25</sub> H <sub>30</sub> O <sub>7</sub>	122215475		[25]
3	Rhodomyrtosone B	Phenolic	C <sub>26</sub> H <sub>34</sub> O <sub>6</sub>	56588580		[25]
4	Tomentosone A	Phenolic	C <sub>41</sub> H <sub>52</sub> O <sub>9</sub>	56929124		[26]
5	Tomentosin	Tannin	C <sub>15</sub> H <sub>20</sub> O <sub>3</sub>	155173		[27]
6	Rhodomyrtial A	Terpenoid	C <sub>45</sub> H <sub>68</sub> O <sub>6</sub>	132513224		[28]
7	Rhodomyrtial B	Terpenoid	C <sub>45</sub> H <sub>68</sub> O <sub>6</sub>	132513225		[28]
8	Tomentodione E	Terpenoid	C <sub>30</sub> H <sub>42</sub> O <sub>3</sub>	132576365		[14], [29]
9	Myricetin	Flavanoid	C <sub>20</sub> H <sub>18</sub> O <sub>12</sub>	14524431		[30]
10	Lupeol	Terpenoid	C <sub>30</sub> H <sub>50</sub> O	259846		[31]

**Table 1:** (Continued)

No	Ligand	Classification	Formulas	Pubchem ID	2D Structure	Ref
11	Alpha Pinene	Essential Oil	C <sub>10</sub> H <sub>16</sub>	6654		[30]
12	Beta Pinene	Essential Oil	C <sub>10</sub> H <sub>16</sub>	14896		[30]
13	Coenzym B	Natural Ligand	C <sub>11</sub> H <sub>22</sub> NO <sub>7</sub> PS	5462265		[10], [32]



**Figure 2:** The active site of MCR a). The active site pocket is highlighted in red and has a surface area of 1986.38 Å<sup>2</sup> and a volume of 1797.40 Å<sup>3</sup>. b). Surface representation of MCR Enzyme with highlighting the binding pocket in white. c). Close-up view of the active site pocket of the MCR enzyme. d). Visualization of the ligand interaction with the MCR enzyme, surrounded by key amino acid residues.

### 2.2.2 Molecular docking and visualization

Molecular docking was simulated using the Autodock Vina in PyRx v08 software to find the best mode. Autogrid was used to determine the grid box in this molecular docking procedure. Ligand was docked using the blind docking method to optimize the potential binding site. The MCR protein has a binding pocket with an area of 1986.382 Å<sup>2</sup> and a volume of 1787.405 Å<sup>3</sup>, as shown in Figure 2. Each ligand was docked 10 times against the MCR target protein.

The docking results are evaluated based on binding affinity and RMSD value. Binding affinity is calculated based on the value of binding free energy (kcal/mol), and the RMSD value is the key in evaluating the docking results. RMSD value is one of the recognized parameters to evaluate the performance of molecular dynamics. An RMSD value (upper bound) with less than 2.0 Å is recommended. Regarding docking accuracy, an RMSD value (upper bound) between 1.0 and 3.0 Å is usually considered a successful docking work [33]. Based on these

parameters, we select the best mode with the smallest binding free energy and an RMSD value below 3.0 Å.

The Pymol visualization tools and Discovery Studio were used to visualize the best mode selected. The visualization shows the bond between the ligand and its target protein; ligand-protein interactions were made, including hydrogen bond interactions, steric (van der Waals), and electrostatic interactions.

### 2.2.3 *In silico* ADMET prediction

Compounds in the keramunting were predicted for their ADMET features for absorption, distribution, metabolism, excretion, and toxicology. Properties, such as the molecular weight, logP, number of hydrogen bond acceptors, number of hydrogen bond donors, and molar refractivity of the drug candidate water solubility (Log mol/L), lipophilicity (Log Po/w), gastrointestinal (GI) absorption, blood-brain barrier (BBB) permeant, and P-gp substrates were estimated using Swiss ADME web tool (<http://www.swissadme.ch/>) [34], while for toxicology features such as LD50 and Toxicity class using PRO TOX II web tool [35].

### 2.2.4 Molecular dynamic simulation

A molecular dynamics simulation was conducted to find the best compounds from molecular docking results. This approach was used to analyze the ligand consistency and the binding mode stability in the protein's binding pocket [36]. MD simulation was performed via Visual Dynamics, a WEB application for molecular dynamics simulation using GROMACS [37]. Ligand topology was obtained through the ACPYPE tool [38]. The operating parameters were set: water model (TIP3), box type (cubic), and box distance 0.5 nm. The force field employed was AMBER99 for 150 ns.

Simulation trajectories were analyzed with the GROMACS package tools 1. Root-mean-square deviation (RMSD) and root-mean-square fluctuation (RMSF) were calculated separately for each system, fitting their heavy atoms and taking the initial structure of the production dynamics as a reference. Hydrogen bonds (H-bonds) were calculated between protein and ligand complexes. We considered a hit when the distance between two polar heavy atoms with at least one hydrogen atom.

## 2.2 *In vitro* study of gas production

The study used an *in vitro* gas production method based on Menke [39]. Experimental with a randomized block design with one treatment, namely three levels of rhodomyrtone, and each treatment was run *in vitro* three times (as a group/repetition), each duplo. Rhodomyrtone treatment dose P0 0 µg/mL, P1 0.125 µg/mL, P2 0.25 µg/mL.

The research material used a substrate consisting of dwarf elephant grass and concentrate in a ratio of 60–40, and the nutrient content was Crude Protein (CP) 13.8%, Crude Fibre (CF) 24.25%, Crude Fat 4.82%, and TDN 60.7%. Incubation was carried out for 48 h, and gas volume was calculated by observation at 1, 2, 4, 8, 12, 24, 36, and 48 h. Gas chromatography measured methane levels with RT-OBond 30 m capillary column, 0.32 mm ID, 10 µm DF, thermal conductivity detector (TCD). The carrier gas used was helium with a flow rate of 1.5 mL/min at 50 °C and a split ratio of 20. The TCD temperature was operated at 200 °C with a current of 40 mA, and the injector temperature was operated at 100 °C.

The effect of the treatment was analyzed using SAS OnDemand for Academic (<https://welcome.oda.sas.com/>) with the Analysis of Variance (ANOVA) method with rhodomyrtone dose treatment and replication as a fixed factor. At the same time, the variable was observed as the dependent variable. The significance level is set at 5%, and if there is a significant difference, it is followed by the Least Significant Difference (LSD) test.

## 3 Results and Discussion

### 3.1 Molecular docking

MCR is a key enzyme in methane formation in methanogenesis, used as a receptor in this docking process [40]. MCR consists of 3 different subunits, namely  $\alpha$  (MCRA),  $\beta$  (MCRB), and  $\gamma$  (MCRG). The three subunits are tightly bound to each other with only 50 Å long hydrophobic channels, which start from the surface and end with a narrow pocket containing the coenzyme F430 in the active site [41], [42]. The last stage of methanogenesis in hydrogenotrophic methanogens is the reduction of methyl-S-CoM to methane. This reaction is catalyzed by the MCR with coenzyme B as an electron donor and coenzyme F430 as a prosthetic group [43], meanwhile, according to Chen *et al.*, [10], two substrates are involved in the MCR-catalyzed reaction (the methyl donor methyl-CoM and the electron donor CoB) and produce two products (CH<sub>4</sub> and CoM-S-S-

CoB) and the final reaction occurs when the substrate binds to the substrate channel in the active site. Therefore, coenzyme B was used as a natural substrate [32] in this docking and compared with 12 compounds from *R. tomentosa*, both binding affinity parameters and RMSD values.

Molecular docking has several advantages, including the possibility of testing or evaluating many natural compounds as drug candidates, antibiotics, and antimicrobials at low cost [44], so it is widely used in various fields of science, including animal biochemistry [45].

**Table 2:** Docking results against MCR.

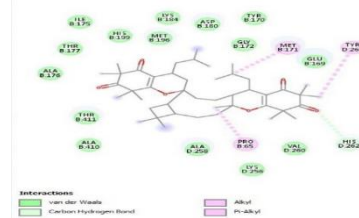
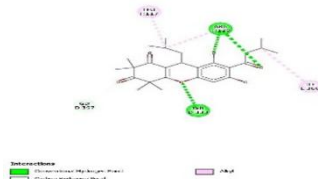
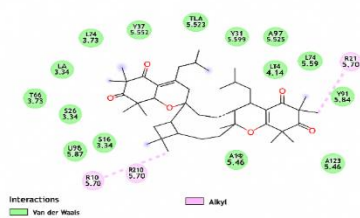
No.	Ligand	Binding Affinity (kcal/mol)	RMSD /ub	RMSD /lb
1	Rhodomtyrtal A	-10.4	9.721	1.863
2	Rhodomtyrtone	-9.5	2.486	1.769
3	Rhodomtyrtal B	-9.3	7.244	3.425
4	Tomentosone A	-9.0	5.925	2.325
5	Rhodomtyrtosone A	-9.0	7.146	2.888
6	Tomentodione E	-8.7	2.11	1.736
7	Myricetin	-8.3	2.578	1.553
8	Lupeol	-8.0	7.73	2.572
9	Rhodomtyrtosone B	-7.8	5.008	1.757
10	Tomentosin	-7.4	4.431	2.715
11	Betapinene	-6.6	19.822	18.345
12	Alphapinene	-6.5	3.27	1.001
13	Coenzyme B	-6.2	2.399	1.913

The blind docking results of 12 compounds and one native substrate using AutodockVina in Pyrex against the MCR protein as the receptor showed diverse results. The docking results in Table 2 were the best mode, selected based on the binding affinity and RMSD values. Based on the data shown (Table 2), 12 compounds' binding affinity ranges from -10.4 to -6.5 kcal/mol, while coenzyme B, a natural substrate,

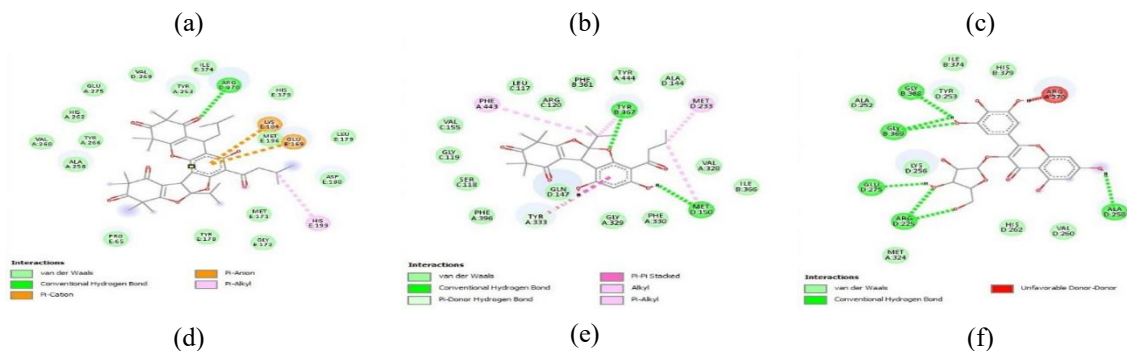
has a score of -6.2 kcal/mol. According to Ika and Hery [46], the binding affinity score is the beginning of the evaluation of a docking process. It estimates the energy required to bind the ligand to the protein. The smaller the binding free energy, the stronger the bond, and this can indicate, which ligand is the strongest from the docking score [47]. So, in this research, all compounds have a high docking score compared to the natural substrate (coenzyme B), above -6.2 kcal/mol. The highest score belongs to Rhodomtyrtal A with -10.4 kcal/mol, and Alpha-pinene with -6.5 kcal/mol has the lowest score.

The RMSD score is a second parameter used to assess this docking process, and an RMSD value (upper bond) between 1.0–3.0 Å is usually considered a successful docking [33]. Only three compounds have RMSD (upper bond) scores below 3.0 Å out of the twelve compounds, namely Rhodomtyrtone, Tomentodione E, and Myricetin, with scores of 2.48 Å, 2.11 Å, and 2.57 Å, respectively, compared to coenzyme B, which has an RMSD score of 2.39 Å. Hence, the result indicates that not all compounds are successfully docked with MCR proteins, even though their binding free energy fulfills the criteria compared to the natural substrate. This can be evaluated from the type of bond and interaction formed between the ligand and the receptor protein.

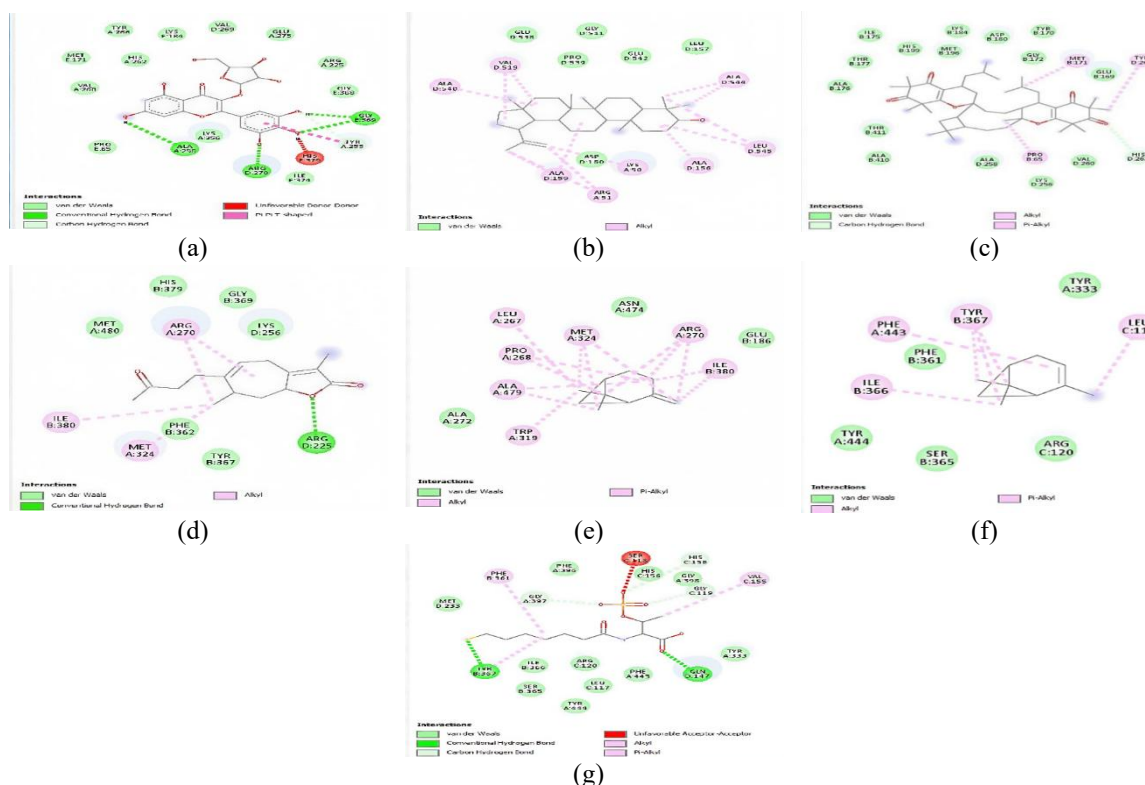
The possible bonds that can be formed, such as hydrogen bond, Van der Waals bond, and hydrophobic bond, are also considered parameters to determine the relationship between structure, activity, and the strength of interaction between atoms, primarily hydrogen and hydrophobic bonds. The interaction of the twelve compounds and one natural substrate with the MCR protein is shown in Figures 3–4 and Table 3.







**Figure 3:** The binding interaction between Rhodomyrtal A (a), Rhodomyrtone (b), Rhodomyrtal B (c), Tomentosone A (d), Rhodomyrtosone A (e), Tomentedione E (f).



**Figure 4:** The binding interaction between Myricetin (a), Lupeol (b), Rhodomyrtosone B (c), Tomentosin (d), Beta-pinene (e), Alpha-pinene (f), Coenzyme B(g).

**Table 3:** Binding interaction with the MCR Protein.

Ligand	Pubchem ID	Hydrogen Bond Interaction		Hydrophobic Interaction	
		NHB	Amino Acid Residues	Interaction	Amino Acid Residues
1 Rhodomyrtal A	132513224	–	TYR D:133, ARG	2	PRO E:65, ARG D:270
2 Rhodomyrtone	44237956	4	F:120 (2), GLY D:397	3	ARG F:120, LEU F:117, ILE E:366
3 Rhodomyrtal B	132513225	1	HIS D:262	3	PRO B:65, MET B:171, TYR D:266
4 Tomentosone A	56929124	1	ARG D:270	3	HIS E:199, GLU E:169, LYS E:187
5 Rhodomyrtosone A	122215475	2	MET D:150, TYR B:367	5	PHE A:443, MET D:233, TYR A:333, MET D:150, TYR B:367
6 Tomentodione E	132576365	7	ARG D:225 (2), GLU D:275, ALA D:256, GLY B:369 (2), GLY B:368	–	
7 Myceretin	14524431	5	ALA A:258, ARG D:270, GLY E:369 (2), TYR A:253	1	TYR A:253
8 Lupeol	259846	–		12	ALA D:540, ALA D:159, ALA D:156, LYS A:50, ARG A:51 (2), LEU D:545 (2), ALA D:544(2), VAL D:519(2)
9 Rhodomyrtosone B	56588580	2	LYS A:256, ARG D:270	2	TYR A:253, LYS A:256
10 Tomentosin	155173	1	ARG D:225	4	ARG A:270 (2), ILE B:380, MET A:324
11 Betapinene	14896	–		14	TRP A:319, LEU A:267, ALA A:479 (2), PRO A:269 (2), ILE B:360 (2), MET A:324 (3), ARG A:270 (3)
12 Alphapinene	6654	–		6	ILE B:366, PHE A:443, TYR B:367 (3), LEU C:117
13 Coenzyme B	5462265	5	TYR B:367, GLN D:147, GLY A:397, GLY C:119, C:158	3	TYR B:367, PHE B:361, VAL C:155

The docking results of 12 compounds from *R. tomentosa* are visualized in 2D using Biovia Discovery Studio Visualizer to show the bonds and interactions that occur. Table 3 shows the type of bond and the number of bonds that emerged from the docking process that was carried out.

The two types of interactions shown in Table 3 are essential because hydrogen bonds and hydrophobic interactions contribute to the mechanical stability of most protein domains [48]. Hydrogen bonds play an essential role in the structure of the complex between ligands and proteins [49]–[51]. The more hydrogen bonds indicate the stronger the interaction between the ligand and protein, because hydrogen bonds make the bond between the two more stable [52], [53]. The more amino acids that bind with hydrogen bonds, the stronger the binding affinity and the smaller the energy required for the interaction between ligands and proteins [54]. The stronger the hydrogen bond, the closer it gets to perfect geometry [55]. It can be said that hydrogen bonds are stronger than hydrophobic

bonds, although both have a crucial role in the bond between ligand and protein.

The molecular docking results have shown that there were three compounds, namely Rhodomyrtone, Tomentodione E, and Myceretin, which have the most hydrogen bonds and are equal to or even higher than the hydrogen bonds possessed by coenzyme B as a natural substrate. Rhodomyrtone has four hydrogen bonds with amino acid residues: TYR D:133, ARG F:120, ARG F:120, GLY D:397, and three hydrophobic bonds (Figure 4). Tomentodione has the most number of hydrogen bonds, which is seven bonds with amino acid residues such as ARG D:225, two bonds, GLU D:275, ALA D:256, GLY B:369, and two bonds, GLY B:368. Myceretin has five hydrogen bonds with amino acid residues: ALA A:258, ARG D:270, GLY E:369 2 bonds, TYR A:253, and one hydrophobic bond. While coenzyme B, as a natural substrate, has five hydrogen bonds with amino acid residues in the form of TYR B: 367, GLN D: 147, GLY A: 397, GLY C: 119, HIS C: 158. The three compounds have the strongest ligand-protein bond as



indicated by the number of hydrogen bonds, but this also follows the small binding affinity value and RMSD below 2.5 Å.

### 3.2 ADMET Prediction

The ADMET prediction study aims to find the properties in the form of predictive models for physicochemical properties, pharmacokinetics, drug-likeness, medicinal chemistry friendliness, and toxicity. According to Lipinski's Rule of Five (RO5), a compound is considered a promising drug candidate for pre-clinical studies if it meets the following criteria: its molecular weight is 500 Dalton or less, it has no more than 10 rotatable bonds, it contains no more than 10 hydrogen bond acceptors, it has no more

than five hydrogen bond donors, and its partition coefficient (log P o/w) is five or less [56], [57].

Based on these criteria, almost all compounds fulfil the criteria to become drug candidates. Table 4 shows three compounds whose molecular weights exceed the criteria: tomentosone A, rhodomyrtal A, and rhodomyrtal B. As for the number of violations, three compounds score 2, namely maceration, rhodomyrtal A, and B. Myricetin also has hydrogen bond acceptor and donor, exceeding the criteria. Hence, the three compounds, namely Myricetin and rhodomyrtal A and B, need more attention if developed as drug candidates. The results shown in Table 4 show that Rhodomyrtone, rhodomyrtosone A and B, and tomentosone show promising results as drug candidates.

**Table 4:** ADME Prediction using the SwissADME web tool.

Compound	M.wt	HBA	HBD	NRB	MF	TPSA	Log P	Log S	GI Absorb	BBB P	B Score	Lipinski's violation
Rhodomyrtone	442.54	6	2	5	124.2	100.9	3.7	-6.02	High	No	0.56	0
Rhodomyrtosone A	442.5	7	2	4	118.4	110.1	3.5	-5.38	High	No	0.56	0
Rhodomyrtosone B	442.54	6	2	5	124.2	100.9	2.9	-6.02	High	No	0.56	0
Tomentosone A	688.85	9	1	6	190.3	133.3	5.1	-9.15	Low	No	0.56	1
Tomentosin	248.32	3	0	3	70.5	43.37	2.4	-2.38	High	Yes	0.55	0
Rhodomyrtal A	705.02	6	0	4	206.5	86.74	4.8	-10.53	Low	No	0.56	2
Rhodomyrtal B	705.02	6	0	4	206.5	86.74	4.8	-10.53	Low	No	0.56	2
Tomentodione E	450.65	3	0	3	136.3	43.37	7.1	-7.23	Low	No	0.85	1
Myricetin	450.35	12	8	4	106.2	210.5	0.4	-3.13	Low	No	0.17	2
Lupeol	426.72	1	1	1	135.1	20.23	6.9	-8.64	Low	No	0.55	1
Alpha Pinene	136.23	0	0	0	45.2	0	4.29	-3.15	Low	Yes	0.55	1
Beta Pinene	136.23	0	0	0	45.2	0	4.29	-3.31	Low	Yes	0.55	1

**Abbreviations:** M.wt = Molecular Weight; HBA = Hydrogen bond acceptor; HBD = Hydrogen bond donor; NRB = Number of rotatable bond; MF = Molar refractivity; TPSA = Topology polar surface area; Log P: Partition coefficient; Log S: Solubility; GI Absorb = Gastrointestinal absorption; BBB P = Blood –brain barrier permeability; B Score = Bioavailability score.

**Table 5:** Toxicology properties.

Compound	LD50	Toxicity Class
Rhodomyrtone	690	4
Rhodomyrtosone A	340	4
Rhodomyrtosone B	690	4
Tomentosone A	838	4
Tomentosin	1330	4
Rhodomyrtal A	1100	4
Rhodomyrtal B	1100	4
Tomentodione E	9500	6
Myricetin	159	3
Lupeol	2000	4
Alpha Pinene	3700	5
Beta Pinene	4700	5

The Pro-Tox II web server was used to predict the toxicological properties of the compounds, with the results presented in Table 5. The predicted oral toxicity of the compounds ranged from 159 mg/kg to 9500 mg/kg. Myricetin, being the only compound with the lowest toxicology class of 3, has a possibility of

toxicity if swallowed. While most other compounds have a toxicity class of 4, there is a possibility of harm if swallowed. Including rhodomyrtone, none of the screened compounds were predicted to be a severe, fatal toxic class (Class I or II). So they can be used as feed.

Based on the results of the ADMET Prediction study, the compound with the best potential that can be used as an inhibitor of MCR enzymes in cattle is rhodomyrtone.

### 3.3 Molecular dynamic simulation

After the docking study, MD simulations were performed to analyze the stability of the best-performing compounds. Molecular dynamics of the protein-ligand complex aid in understanding the flexibility and conformational variations and the molecular basis of inhibition. We assessed binding

affinity and system stability using RMSD, RMSF, Rg, H-bond, and solvent accessible surface area (SASA) parameters to identify the optimal complex [58]. These analyses are essential for understanding the dynamic behavior of proteins over various timescales, from rapid internal movements to slower structural changes and protein folding. Based on a physics model of interactions, this method predicts atomic movements over time and captures critical molecular processes such as ligand binding, protein deformation, and folding with femtosecond resolution [59].

Rhodomlyrtone was selected based on the molecular docking results for MD simulation of the protein-ligand complex. The MD simulation of the protein-ligand complex between rhodomlyrtone and MCR subunit alpha protein was performed for 150 ns. As shown in Figure 5, the RMSD value in this simulation was recorded between 0.15 nm and 0.2 nm at the end of the 150 ns simulation. At the beginning of the simulation, the RMSD value rises from 0.15 to 0.2 nm at 0 to 10 ns and then stabilises until the end

with a value of 0.2 nm. The bonding can be robust when viewed from the low RMSD value. In computer-aided drug design, calculating the RMSD is a conventional method for evaluating structural alterations of a macromolecule during molecular dynamics simulations [60].

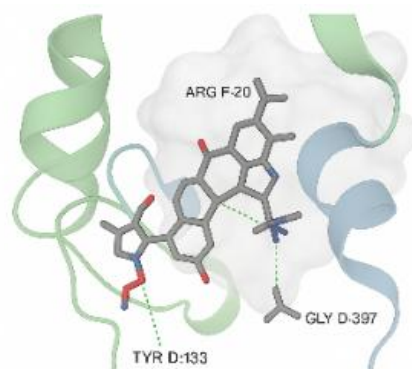


Figure 5: Amino acid residues of rhodomlyrtone.

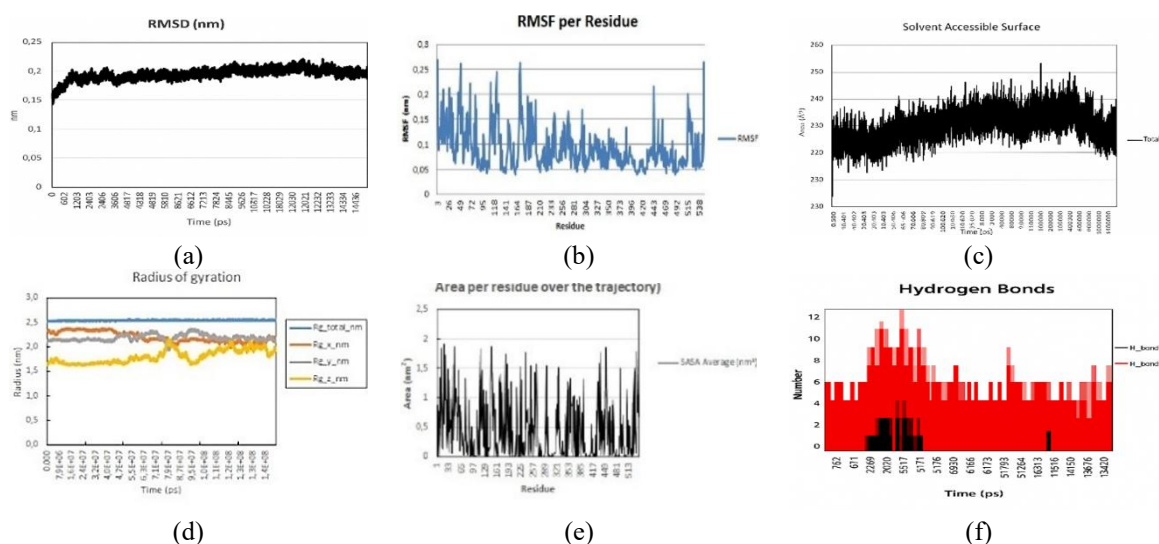


Figure 6: Molecular dynamic simulation of rhodomlyrtone against the MCR subunit alpha enzyme (a) RMSD, (b) RMSF, (c) SAS, (d) Rg, (e) Area per residue, (f) Hydrogen bonds.

The stability of protein ligand-complex can be evaluated from the RMSF that represented the binding fluctuation between protein residue and ligand [61]. In this study, the RMSF value of protein-ligand complex exhibited exclusive fluctuation in various ranges, from the first residue to 200 the RMSF value is in the range of 0.05–0.25 nm, from 250–400 the value is in the range of 0.05–0.175, and the rest of the residues exhibited the RMSF value in the range of 0.05–0.25.

However, the MCR subunit alpha enzyme shows a low RMSF value ( $\leq 2.5$  nm) for the residue of the binding site or predicted catalytic site, indicating strong molecular interaction between the protein enzyme and ligand [62].

The radius of gyration (Rg) represents the compactness of the protein-ligand complex, with a smaller Rg value indicating a more compact structure [63]. In our study, Rg of the protein and ligand

complexes was initially found to be between 2.5 and 2.6 nm. The  $R_g$  values of the main protease with amodiaquine were stabilized after five ns, indicating a stable binding pose. This confirms a plateau formed in the  $R_g$  curve, indicating that the protein had been folded well [64].

Stability of protein-ligand complexes can be inspected by calculating the number of intermolecular hydrogen bonds [65]. Hydrogen bond analysis can determine the binding mode and interaction between the protein and ligand. The hydrogen plot shows two types of bonding distance: hydrogen bonding distance within 0.35 nm represents the stronger bonding, and hydrogen bonding distance greater than 0.35 nm represents the weaker bonding [61]. The intermolecular hydrogen bond between the MCR subunit alpha enzyme and rhodomyltone was depicted in Figure 5. Based on the MD simulation, three hydrogen bonds were consistently observed throughout the MD simulation, while a maximum of eight hydrogen bonds were observed at different time frames. The plot shows that hydrogen bonds were dominated by bonds with a length of less than 0.35 nm, indicating a strong interaction between the MCR subunit alpha enzyme and rhodomyltone.

The SASA was performed to analyse the portion of the protein that is exposed and interacts with the surrounding solvent, indicating the stability and folding of the protein [62]. The result of the SASA plot is depicted in Figure 6. The results show that the traces for the SASA value steeped up within 125 ns, indicating protein structure relaxation and potentially reducing protein stability.

### 3.4 *In vitro* gas production

Based on the *in silico* screening of twelve bioactive compounds from *R. tomentosa*, Rhodomyltone demonstrated the most promising inhibitory interaction with the MCR enzyme. It exhibited a strong binding affinity of -9.5 kcal/mol and an RMSD value of 2.48 Å, both indicating a stable and accurate binding pose (Table 2) [33], [46]. Rhodomyltone also formed four hydrogen bonds with key active site residues such as TYR D:133 and ARG F:120, supporting its potential as a competitive MCR inhibitor (Table 3) [48], [54]. ADMET predictions confirmed its drug-likeness with no Lipinski's rule violations, high gastrointestinal absorption, and low predicted toxicity ( $LD_{50}$  = 690 mg/kg, toxicity class 4), making it a safe candidate for feed-based applications [34], [35], [56]. Furthermore, molecular dynamics

simulations over 150 ns showed that the rhodomyltone-MCR complex remained stable throughout, with low RMSD values (0.15–0.20 nm), stable radius of gyration (2.5–2.6 nm), and consistent hydrogen bonding (3–8 bonds within  $\leq 0.35$  nm), indicating strong and sustained binding interactions [58], [60], [61], [65].

The combined docking and molecular dynamic simulation evidence supports rhodomyltone as a prioritized lead for MCR inhibitor, as it demonstrated strong binding affinity, stable interaction with conserved active-site residues, and sustained structural stability during long-timescale simulation [66], [67]. These results and favorable ADMET predictions highlight rhodomyltone as a promising candidate for further validation. These computational findings provided a robust basis to advance rhodomyltone into *in vitro* evaluation. Using a rumen fermentation model, the compound's efficacy in reducing methane production was tested at sub-MIC concentrations (0.125 and 0.25  $\mu\text{g/mL}$ ), following previous MIC reports of 0.5–1  $\mu\text{g/mL}$  [68]. This approach aimed to verify whether the predicted molecular inhibition of MCR could translate into measurable methane reduction without broadly disrupting rumen microbial activity. The test was conducted in 3 runs with two replicates of each run for each treatment.

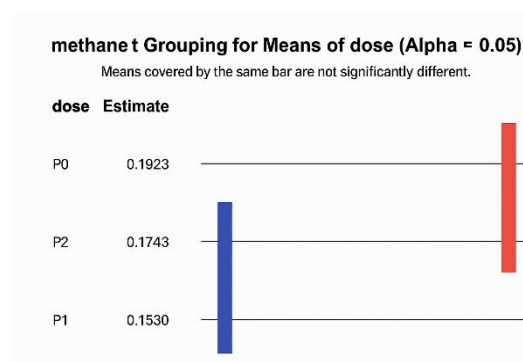
Gas production is closely related to the methane and  $\text{CO}_2$  generated during the fermentation process by rumen microbes. In this experiment, adding rhodomyltone did not significantly affect methane production at 0.125  $\mu\text{g/mL}$  and 0.25  $\mu\text{g/mL}$  doses. Methane production in P0 (without rhodomyltone) was recorded at 0.192 ml/mg of dry matter digested, while in P1 (dose 0.125  $\mu\text{g/mL}$ ) it was 0.153 ml/mg of dry matter digested, and in P2 (dose 0.25  $\mu\text{g/mL}$ ) it was 0.174 ml/mg of dry matter digested. Statistical analysis shown in Table 6 showed no significant difference from the control ( $p$ -values  $> 0.05$ ). However, a downward trend (Figure 7) indicates that increasing the dose led to a gradual reduction in methane production. Numerically, methane output decreased by approximately 10% compared to the control (P0). Although the statistical analysis revealed no significant difference among the treatments, the reduction pattern suggests a potential inhibitory effect of the treatment on methanogenesis activity. This decrease may be attributed to the suppression of methanogenic archaea or the inhibition of key enzymatic pathways such as MCR, which plays a central role in the final step of methane biosynthesis.

Furthermore, their effects are dose-dependent, as varying concentrations can influence the magnitude of methane reduction and overall rumen function. Therefore, optimizing the type and dosage of bioactive compounds is essential to achieve effective and sustainable methane mitigation in ruminant systems. The dose-dependent response implies that higher concentrations of bioactive compounds may gradually alter the structure of the rumen microbial community, shifting hydrogen utilization toward alternative pathways such as propionate formation instead of methanogenesis [69], [70].

**Table 6:** *In vitro* study results of methane production

Block	Methane production (mL/mg)			p-values
	P0	P1	P2	
1	0,285	0,264	0,275	
2	0,185	0,112	0,143	
3	0,107	0,083	0,105	
Means	0,192 <sup>a</sup>	0,153 <sup>a</sup>	0,174 <sup>a</sup>	0,08*

\*Means with the same letter are not significantly different.



**Figure 7:** Methane production (ml/mg of dry matter (digested), between treatments. Blue bar : P2 vs P1, Red Bar: P0 vs P2, Different colors represent significantly different means.

Methane is produced as a byproduct of feed fermentation, particularly the fermentation of carbohydrates into VFAs (acetate, propionate, butyrate). In the ruminant metabolism pathway, the production of acetate and butyrate releases pure hydrogen, while propionate formation creates a competitive pathway for using  $H^+$  in the rumen [68]. Methanogens in the rumen act as decomposers of hydrogen ( $H_2$ ) and  $CO_2$  produced by other microbes during feed fermentation, using them to produce  $CH_4$  and help maintain lower reductive conditions to allow other microbial metabolic processes [71].

Rhodomyltone in this study was used to mitigate methane production by leveraging its antimicrobial properties, as demonstrated in several previous studies against various types of bacteria, especially gram-positive bacteria [16], [24], [72]. Antimicrobial compounds aim to manipulate rumen microbes associated with  $CH_4$  formation. Previous research has shown that antimicrobial compounds can reduce methane production by inhibiting methanogens directly or indirectly [73], [74]. Plant-derived phenolic compounds have been shown to reduce methane production in ruminants. The phenolic compound reduced methane production by suppressing methanogens and protozoa, also demonstrated antimethanogenic activity by altering rumen fermentation and microbial population [75]–[77]. Together, these findings highlight that rhodomyltone, like other phenolic compounds, might inhibit methanogen activity by directly affecting methanogen populations or by reducing the availability of molecular hydrogen through the reduction of protozoa. The antimicrobial activity of rhodomyltone is expected to inhibit methanogen activity directly, reduce protozoan growth, and decrease the activity of  $H_2$ -producing bacteria due to their role in producing  $H_2$  when breaking down cellulose into VFAs [9], [78], thus hindering  $CH_4$  formation.

However, this antimicrobial activity did not directly affect methanogens, likely because the treatment dose was not strong enough to suppress them. The doses used in this study were based on the minimum inhibitory concentration (MIC) of rhodomyltone, which is 0.5-1  $\mu\text{g/ml}$  [72]. MIC is the minimum concentration an antimicrobial needs to inhibit a microbe fully.

This study used  $\frac{1}{4}$  and  $\frac{1}{2}$  MIC doses with the hope that not all rumen bacteria would be suppressed, which could disrupt fermentation processes in the rumen. With this approach, the doses used were insufficient to inhibit methanogen activity maximally.

#### 4 Conclusions

This study demonstrated that several bioactive compounds from *R. tomentosa* possess promising inhibitory potential against the key methanogenesis enzyme methyl-coenzyme M reductase (MCR). Among the twelve compounds analyzed through molecular docking, rhodomyltone showed the most favorable interaction profile, with strong binding

affinity, optimal RMSD values, and multiple hydrogen bonds with critical active site residues. ADMET predictions further supported rhodomyrton's suitability as a safe and drug-like compound. Molecular dynamics simulations confirmed the stability and persistence of rhodomyrton binding over 150 ns, reinforcing its potential as a robust enzyme inhibitor.

*In vitro* evaluation using rumen fermentation models indicated that rhodomyrton could reduce methane production by approximately 10% at sub-MIC concentrations. While this decline did not attain statistical significance, the observed downward trend suggests functional relevance and warrants further investigation. The absence of statistical significance may be ascribed to numerous factors, including the limited sample size, the substantial variability among rumen microbial populations, and the potential for confounding variables inherent in the fermentation system. These considerations underscore the necessity for more robust experimental designs in future studies. In summary, the results of the study indicate that rhodomyrton is a potential agent for methane mitigation in ruminants. Subsequent research should concentrate on optimizing dosage, exploring synergistic effects with other bioactive compounds, and conducting *in vivo* trials to validate its efficacy under practical feeding conditions.

### Acknowledgments

This research was funded by grants from the RTA (Rekognisi Tugas Akhir) 2023 program at Gadjah Mada University.

### Author Contributions

Conceptualization: S.P., A.K., M.M., F.B.Z.; Methodology: S.P., H.L.S., F.B.Z.; Writing-original draft preparation: S.P., B.H., Y.N.A., N.H.K., W.W.; Validation: M.M., A.K., M.A.A., B.S., B.H., Y.N.A., S.W., S.S., W.W.; Formal analysis: S.P., W.W., S.W., H.L.S., B.H.; Investigation: S.P., A.K., M.M., M.A.A., B.S., F.B.Z.; Review and editing: S.P., B.H., A.K., M.M., M.A.A., B.S., Y.N.A., W.W., S.S., F.B.Z. All authors have read and agreed to the published version of the manuscript.

### Conflicts of Interest

The authors declare no conflict of interest.

### References

- [1] Food and Agriculture Organization (FAO), *Methane Emissions in Livestock and Rice Systems*. Rome, Italy: FAO, 2023, doi: 10.4060/cc7607en.
- [2] A. M. Dlamini and M. A. Dube, "Contribution of animal agriculture to greenhouse gases production in Swaziland," *American Journal of Climate Change*, vol. 3, no. 3, pp. 253–260, 2014, doi: 10.4236/ajcc.2014.33024.
- [3] M. M. Rojas-Downing, A. P. Nejadhashemi, T. Harrigan, and S. A. Woznicki, "Climate change and livestock: Impacts, adaptation, and mitigation," *Climate Risk Management*, vol. 16, pp. 145–163, 2017, doi: 10.1016/j.crm.2017.02.001.
- [4] KLHK, *Laporan Inventarisasi GRK 2020 dan Monitoring, Pelaporan, Verifikasi (MPV)*, Kementerian Lingkungan Hidup dan Kehutanan, pp. 1–143, 2020.
- [5] A. Chaokaur, T. Nishida, I. Phaowphaisal, and K. Sommart, "Effects of feeding level on methane emissions and energy utilization of Brahman cattle in the tropics," *Agriculture, Ecosystems & Environment*, vol. 199, pp. 225–230, 2015, doi: 10.1016/j.agee.2014.09.014.
- [6] B. H. Khairunisa, C. Heryakusuma, K. Ike, B. Mukhopadhyay, and D. Susanti, "Evolving understanding of rumen methanogen ecophysiology," *Frontiers in Microbiology*, vol. 14, Nov. 2023, doi: 10.3389/fmicb.2023.1296008.
- [7] M. B. Eisen and P. O. Brown, "Rapid global phaseout of animal agriculture has the potential to stabilize greenhouse gas levels for 30 years and offset 68 percent of CO<sub>2</sub> emissions this century," *PLOS Climate*, vol. 1, no. 2, p. e0000010, Feb. 2022, doi: 10.1371/journal.pclm.0000010.
- [8] K. Singh et al., "Molecular identification of methanogenic archaea from Surti buffaloes (*Bubalus bubalis*) reveals more hydrogenotrophic methanogen phylotypes," *Brazilian Journal of Microbiology*, vol. 42, no. 1, pp. 132–139, Mar. 2011, doi: 10.1590/S1517-83822011000100017.
- [9] A. Patra, T. Park, M. Kim, and Z. Yu, "Rumen methanogens and mitigation of methane emission by anti-methanogenic compounds and substances," *Journal of Animal Science and*

- Biotechnology*, vol. 8, no. 1, p. 13, Dec. 2017, doi: 10.1186/s40104-017-0145-9.
- [10] H. Chen, Q. Gan, and C. Fan, "Methyl-coenzyme M reductase and its post-translational modifications," *Frontiers in Microbiology*, vol. 11, Oct. 2020, doi: 10.3389/fmicb.2020.578356.
- [11] A. Gendron and K. D. Allen, "Overview of diverse methyl/alkyl-coenzyme M reductases and considerations for their potential heterologous expression," *Frontiers in Microbiology*, vol. 13, Apr. 2022, doi: 10.3389/fmicb.2022.867342.
- [12] J. C. Ku-Vera et al., "Role of secondary plant metabolites on enteric methane mitigation in ruminants," *Frontiers in Veterinary Science*, vol. 7, Aug. 2020, doi: 10.3389/fvets.2020.00584.
- [13] C. Narabe et al., "Cashew nut shell liquid potentially mitigates methane emission from the feces of Thai native ruminant livestock by modifying fecal microbiota," *Animal Science Journal*, vol. 92, no. 1, Jan. 2021, doi: 10.1111/asj.13614.
- [14] Y.-L. Zhang et al., "Isolation, structure elucidation, and absolute configuration of syncarpic acid-conjugated terpenoids from *Rhodomyrtus tomentosa*," *Journal of Natural Products*, vol. 80, no. 4, pp. 989–998, Apr. 2017, doi: 10.1021/acs.jnatprod.6b01005.
- [15] D. Jeong et al., "In vitro and in vivo anti-inflammatory effect of *Rhodomyrtus tomentosa* methanol extract," *Journal of Ethnopharmacology*, vol. 146, no. 1, pp. 205–213, Mar. 2013, doi: 10.1016/j.jep.2012.12.034.
- [16] Q. N. Bach et al., "Antimicrobial activity of rhodomyrtone isolated from *Rhodomyrtus tomentosa* (Aiton) Hassk," *Natural Product Research*, vol. 34, no. 17, pp. 2518–2523, Sep. 2020, doi: 10.1080/14786419.2018.1540479.
- [17] O. F. Nwabor, S. Leejae, and S. P. Voravuthikunchai, "Rhodomyrtone accumulates in bacterial cell wall and cell membrane and inhibits the synthesis of multiple cellular macromolecules in epidemic methicillin-resistant *Staphylococcus aureus*," *Antibiotics*, vol. 10, no. 5, 2021, doi: 10.3390/antibiotics10050543.
- [18] S. Wunoo, J. Saising, and S. P. Voravuthikunchai, "Rhodomyrtone inhibits lipase production, biofilm formation, and disorganizes established biofilm in *Propionibacterium acnes*," *Anaerobe*, vol. 43, pp. 61–68, Feb. 2017, doi: 10.1016/j.anaerobe.2016.12.002.
- [19] H.-X. Liu et al., "Rhodomentones A and B, novel meroterpenoids with unique NMR characteristics from *Rhodomyrtus tomentosa*," *Organic & Biomolecular Chemistry*, vol. 14, no. 30, pp. 7354–7360, 2016, doi: 10.1039/C6OB01215A.
- [20] W. Mitsuwan, P. Wintachai, and S. P. Voravuthikunchai, "Rhodomyrtus tomentosa leaf extract and rhodomyrtone combat *Streptococcus pneumoniae* biofilm and inhibit invasiveness to human lung epithelial and enhance pneumococcal phagocytosis by macrophage," *Current Microbiology*, vol. 77, no. 11, pp. 3546–3554, Nov. 2020, doi: 10.1007/s00284-020-02164-3.
- [21] S. Puspito et al., "Phytochemical diversity, rhodomyrtone content, nutrient content, and antioxidant efficacy in *keramunting* leaves from Belitung Island, Indonesia: A comparative study of different solvent extraction methods," *Case Studies in Chemical and Environmental Engineering*, vol. 10, Jun. 2024, p. 100874, doi: 10.1016/j.cscee.2024.100874.
- [22] L. D. Saravolatz and J. Pawlak, "Rhodomyrtone: A new anti-*Staphylococcus aureus* agent against resistant strains," *JAC-Antimicrobial Resistance*, vol. 6, no. 4, pp. 1–4, 2024, doi: 10.1093/jacamr/dlae097.
- [23] W. R. Mir et al., "Molecular docking analysis and evaluation of the antimicrobial properties of the constituents of *Geranium wallichianum* D. Don ex Sweet from Kashmir Himalaya," *Scientific Reports*, vol. 12, no. 1, p. 12547, Jul. 2022, doi: 10.1038/s41598-022-16102-9.
- [24] Dachriyanus et al., "Rhodomyrtone, an antibiotic from *Rhodomyrtus tomentosa*," *Australian Journal of Chemistry*, vol. 55, no. 3, pp. 229–232, 2002, doi: 10.1071/CH01194.
- [25] A. Gervais, K. E. Lazarski, and J. A. Porco, "Divergent total syntheses of rhodomyrtosones A and B," *Journal of Organic Chemistry*, vol. 80, no. 19, pp. 9584–9591, Oct. 2015, doi: 10.1021/acs.joc.5b01570.
- [26] A. Hiranrat, W. Mahabusarakam, A. R. Carroll, S. Duffy, and V. M. Avery, "Tomentosones A and B, hexacyclic phloroglucinol derivatives from the Thai shrub *Rhodomyrtus tomentosa*," *Journal of Organic Chemistry*, vol. 77, no. 1, pp. 680–683, Jan. 2012, doi: 10.1021/jo201602y.
- [27] L. Yanze, H. Aijun, J. Chunru, and W. Yangjie, "Isolation and structure of hydrolysable tannins from *Rhodomyrtus tomentosa*," *Natural Product*



- Research and Development*, vol. 10, no. 1, pp. 14–19, 1998.
- [28] Y.-L. Zhang et al., “Rhodomyrtals A and B, two meroterpenoids with a triketone–sesquiterpene–triketone skeleton from *Rhodomyrtus tomentosa*: Structural elucidation and biomimetic synthesis,” *Organic Letters*, vol. 18, no. 16, pp. 4068–4071, Aug. 2016, doi: 10.1021/acs.orglett.6b01944.
- [29] H.-X. Liu, H.-B. Tan, and S.-X. Qiu, “Antimicrobial acylphloroglucinols from the leaves of *Rhodomyrtus tomentosa*,” *Journal of Asian Natural Products Research*, vol. 18, no. 6, pp. 535–541, Jun. 2016, doi: 10.1080/10286020.2015.1121997.
- [30] T. Vo and D. Ngo, “The health beneficial properties of *Rhodomyrtus tomentosa* as potential functional food,” *Biomolecules*, vol. 9, no. 2, p. 76, Feb. 2019, doi: 10.3390/biom9020076.
- [31] H. Wai-Haan and L. Man-Moon, “Two new triterpenoids from *Rhodomyrtus tomentosa*,” *Phytochemistry*, vol. 15, no. 11, pp. 1741–1743, Jan. 1976, doi: 10.1016/S0031-9422(00)97468-5.
- [32] T. Wongnate and S. W. Ragsdale, “The reaction mechanism of methyl-coenzyme M reductase,” *Journal of Biological Chemistry*, vol. 290, no. 15, pp. 9322–9334, Apr. 2015, doi: 10.1074/jbc.M115.636761.
- [33] M. Nabil, R. Alam, Q. A. Rahman, M. M. Ul Islam, and M. A. A. Noor, “*In silico* molecular docking study of some already approved antiviral drugs, vitamins and phytochemical components against RNA dependent RNA polymerase of SARS-CoV-2 virus,” *Journal of Applied Bioinformatics and Computational Biology*, vol. 9, no. 5, 2020, doi: 10.37532/jabcb.2020.9(5).182.
- [34] A. Daina, O. Michielin, and V. Zoete, “SwissADME: A free web tool to evaluate pharmacokinetics, drug-likeness and medicinal chemistry friendliness of small molecules,” *Scientific Reports*, vol. 7, no. 1, p. 42717, Mar. 2017, doi: 10.1038/srep42717.
- [35] P. Banerjee, A. O. Eckert, A. K. Schrey, and R. Preissner, “ProTox-II: A webserver for the prediction of toxicity of chemicals,” *Nucleic Acids Research*, vol. 46, no. W1, pp. W257–W263, Jul. 2018, doi: 10.1093/nar/gky318.
- [36] W. L. Jorgensen, J. Chandrasekhar, J. D. Madura, R. W. Impey, and M. L. Klein, “Comparison of simple potential functions for simulating liquid water,” *Journal of Chemical Physics*, vol. 79, no. 2, pp. 926–935, Jul. 1983, doi: 10.1063/1.445869.
- [37] I. H. P. Vieira, E. B. Botelho, T. J. de Souza Gomes, R. Kist, R. A. Caceres, and F. B. Zanchi, “Visual dynamics: A web application for molecular dynamics simulation using GROMACS,” *BMC Bioinformatics*, vol. 24, no. 1, p. 107, Mar. 2023, doi: 10.1186/s12859-023-05234-y.
- [38] L. Kagami, A. Wilter, A. Diaz, and W. Vranken, “The ACPYPE web server for small-molecule MD topology generation,” *Bioinformatics*, vol. 39, no. 6, Jun. 2023, doi: 10.1093/bioinformatics/btad350.
- [39] K. H. Menke, L. Raab, A. Salewski, H. Steingass, D. Fritz, and W. Schneider, “The estimation of the digestibility and metabolizable energy content of ruminant feedingstuffs from the gas production when they are incubated with rumen liquor *in vitro*,” *Journal of Agricultural Science*, vol. 93, no. 1, pp. 217–222, 1979, doi: 10.1017/S0021859600086305.
- [40] N. Shao et al., “Expression of divergent methyl/alkyl coenzyme M reductases from uncultured archaea,” *Communications Biology*, vol. 5, no. 1, 2022, doi: 10.1038/s42003-022-04057-6.
- [41] T. Wagner, C.-E. Wegner, J. Kahnt, U. Ermler, and S. Shima, “Phylogenetic and structural comparisons of the three types of methyl coenzyme M reductase from *Methanococcales* and *Methanobacteriales*,” *Journal of Bacteriology*, vol. 199, no. 16, Aug. 2017, doi: 10.1128/JB.00197-17.
- [42] R. K. Thauer, “Methyl (alkyl)-coenzyme M reductases: Nickel F-430-containing enzymes involved in anaerobic methane formation and in anaerobic oxidation of methane or of short chain alkanes,” *Biochemistry*, vol. 58, no. 52, pp. 5198–5220, Dec. 2019, doi: 10.1021/acs.biochem.9b00164.
- [43] Z. Lyu, N. Shao, T. Akinyemi, and W. B. Whitman, “Methanogenesis,” *Current Biology*, vol. 28, no. 13, pp. R727–R732, Jul. 2018, doi: 10.1016/j.cub.2018.05.021.
- [44] M. C. Vlasiou and K. S. Pafti, “Screening possible drug molecules for COVID-19: The example of vanadium (III/IV/V) complex molecules with computational chemistry and molecular docking,” *Computational Toxicology*, vol. 18, p. 100157, May 2021, doi: 10.1016/j.comtox.2021.100157.

- [45] J. M. Paggi, A. Pandit, and R. O. Dror, "The art and science of molecular docking," *Annual Review of Biochemistry*, vol. 93, no. 1, pp. 389–410, Aug. 2024, doi: 10.1146/annurev-biochem-030222-120000.
- [46] I. N. Fitriani and H. M. Ansory, "Molecular docking study of nutmeg (*Myristica fragrans*) constituents as anti-skin cancer agents," *JKPK (Jurnal Kimia dan Pendidikan Kimia)*, vol. 6, no. 1, p. 14, Apr. 2021, doi: 10.20961/jkpk.v6i1.47223.
- [47] F. Rahman, S. Tabrez, R. Ali, A. S. Alqahtani, M. Z. Ahmed, and A. Rub, "Molecular docking analysis of rutin reveals possible inhibition of SARS-CoV-2 vital proteins," *Journal of Traditional and Complementary Medicine*, vol. 11, no. 2, pp. 173–179, Mar. 2021, doi: 10.1016/j.jtcm.2021.01.006.
- [48] G. G. Ferenczy and M. Kellermayer, "Contribution of hydrophobic interactions to protein mechanical stability," *Computational and Structural Biotechnology Journal*, vol. 20, pp. 1946–1956, 2022, doi: 10.1016/j.csbj.2022.04.025.
- [49] S. J. Grabowski, *Understanding Hydrogen Bonds: Theoretical and Experimental Views*. Cambridge, UK: Royal Society of Chemistry, 2020.
- [50] A. Madushanka, R. T. Moura, N. Verma, and E. Kraka, "Quantum mechanical assessment of protein–ligand hydrogen bond strength patterns: Insights from semiempirical tight-binding and local vibrational mode theory," *International Journal of Molecular Sciences*, vol. 24, no. 7, p. 6311, Mar. 2023, doi: 10.3390/ijms24076311.
- [51] F. K. Malik and J. Guo, "Insights into protein–DNA interactions from hydrogen bond energy-based comparative protein–ligand analyses," *PROTEINS: Structure, Function, and Bioinformatics*, vol. 90, no. 6, pp. 1303–1314, Jun. 2022, doi: 10.1002/prot.26313.
- [52] A. Abelian, M. Dybek, J. Wallach, B. Gaye, and A. Adejare, "Pharmaceutical chemistry," in *Remington*, Amsterdam, Netherlands: Elsevier, 2021, pp. 105–128.
- [53] T. E. Tallei et al., "Potential of plant bioactive compounds as SARS-CoV-2 main protease (Mpro) and spike (S) glycoprotein inhibitors: A molecular docking study," *Scientifica (Cairo)*, vol. 2020, pp. 1–18, Dec. 2020, doi: 10.1155/2020/6307457.
- [54] G. Sanger et al., "Green seaweed *Caulerpa racemosa* – Chemical constituents, cytotoxicity in breast cancer cells and molecular docking simulation," *Journal of Agricultural and Food Research*, vol. 12, p. 100621, Jun. 2023, doi: 10.1016/j.jafr.2023.100621.
- [55] M. M. Hasan et al., "In silico molecular docking and ADME/T analysis of quercetin compound with its evaluation of broad-spectrum therapeutic potential against particular diseases," *Informatics in Medicine Unlocked*, vol. 29, p. 100894, 2022, doi: 10.1016/j.imu.2022.100894.
- [56] M. D. Shultz, "Two decades under the influence of the rule of five and the changing properties of approved oral drugs," *Journal of Medicinal Chemistry*, vol. 62, no. 4, pp. 1701–1714, Feb. 2019, doi: 10.1021/acs.jmedchem.8b00686.
- [57] H. Amat-ur-Rasool et al., "In silico design of dual-binding site anti-cholinesterase phytochemical heterodimers as treatment options for Alzheimer's disease," *Current Issues in Molecular Biology*, vol. 44, no. 1, pp. 152–175, 2022, doi: 10.3390/cimb44010012.
- [58] S. K. Halder et al., "In silico identification and analysis of potentially bioactive antiviral phytochemicals against SARS-CoV-2: A molecular docking and dynamics simulation approach," *BioMed Research International*, vol. 2023, pp. 1–32, May 2023, doi: 10.1155/2023/5469258.
- [59] J. Aghajani et al., "Molecular dynamic simulations and molecular docking as a potential way for designed new inhibitor drug without resistance," *Tanaffos*, vol. 21, no. 1, pp. 1–14, 2022.
- [60] K. Sargsyan, C. Grauffel, and C. Lim, "How molecular size impacts RMSD applications in molecular dynamics simulations," *Journal of Chemical Theory and Computation*, vol. 13, no. 4, pp. 1518–1524, Apr. 2017, doi: 10.1021/acs.jctc.7b00028.
- [61] P. Bisht et al., "Designing of xanthine-based DPP-4 inhibitors: a structure-guided alignment dependent multifacet 3D-QSAR modeling, and molecular dynamics simulation study," *Journal of Biomolecular Structure and Dynamics*, pp. 1–25, May 2024, doi: 10.1080/07391102.2024.2329787.
- [62] H. A. Oyewusi et al., "Bioinformatics analysis and molecular dynamics simulations of azoreductases (AzrBmH2) from *Bacillus megaterium* H2 for the decolorization of

- commercial dyes,” *Environmental Sciences Europe*, vol. 36, no. 1, p. 31, Feb. 2024, doi: 10.1186/s12302-024-00853-5.
- [63] A. Shrestha et al., “Molecular docking and dynamics simulation of several flavonoids predict cyanidin as an effective drug candidate against SARS-CoV-2 spike protein,” *Advances in Pharmacology and Pharmaceutical Sciences*, vol. 2022, pp. 1–13, Nov. 2022, doi: 10.1155/2022/3742318.
- [64] D.-D. Li et al., “Molecular dynamics analysis of binding sites of epidermal growth factor receptor kinase inhibitors,” *ACS Omega*, vol. 5, no. 26, pp. 16307–16314, Jul. 2020, doi: 10.1021/acsomega.0c02183.
- [65] A. M. da Fonseca et al., “Screening of potential inhibitors targeting the main protease structure of SARS-CoV-2 via molecular docking, and approach with molecular dynamics, RMSD, RMSF, H-bond, SASA and MMGBSA,” *Molecular Biotechnology*, Jul. 2023, doi: 10.1007/s12033-023-00831-x.
- [66] A. A. Al-Karmalawy et al., “Molecular docking and dynamics simulation revealed the potential inhibitory activity of ACEIs against SARS-CoV-2 targeting the hACE2 receptor,” *Frontiers in Chemistry*, vol. 9, p. 661230, 2021, doi: 10.3389/fchem.2021.661230.
- [67] O. M. H. Salo-Ahen et al., “Molecular dynamics simulations in drug discovery and pharmaceutical development,” *Processes*, vol. 9, no. 1, p. 71, 2021, doi: 10.3390/pr9010071.
- [68] V. Palangi, M. Macit, H. Nadaroglu, and A. Taghizadeh, “Effects of green-synthesized CuO and ZnO nanoparticles on ruminal mitigation of methane emission to the enhancement of the cleaner environment,” *Biomass Conversion and Biorefinery*, 2022, doi: 10.1007/s13399-022-02775-9.
- [69] D. K. Dhanasekaran et al., “Plants extract and bioactive compounds on rumen methanogenesis,” *Agroforestry Systems*, vol. 94, pp. 1541–1553, 2020, doi: 10.1007/s10457-019-00411-6.
- [70] N. F. Sari, P. Ray, C. Rymer, K. E. Kliem, and S. Stergiadis, “Garlic and its bioactive compounds: Implications for methane emissions and ruminant nutrition,” *Animals*, vol. 12, no. 2998, pp. 1–33, 2022, doi: 10.3390/ani12212998.
- [71] A. K. Patra and R. Puchala, “Methane mitigation in ruminants with structural analogues and other chemical compounds targeting archaeal methanogenesis pathways,” *Biotechnology Advances*, vol. 69, p. 108268, 2023, doi: 10.1016/j.biotechadv.2023.108268.
- [72] O. F. Nwabor, S. Leejae, and S. P. Voravuthikunchai, “Rhodomymrtone accumulates in bacterial cell wall and cell membrane and inhibits the synthesis of multiple cellular macromolecules in epidemic methicillin-resistant *Staphylococcus aureus*,” *Antibiotics*, vol. 10, no. 5, 2021, doi: 10.3390/antibiotics10050543.
- [73] Y. Dinakarkumar et al., “Anti-methanogenic effect of phytochemicals on methyl-coenzyme M reductase—potential: In silico and molecular docking studies for environmental protection,” *Micromachines*, vol. 12, no. 11, 2021, doi: 10.3390/mi12111425.
- [74] V. Palangi and M. Lackner, “Management of enteric methane emissions in ruminants using feed additives: A review,” *Animals*, vol. 12, no. 24, pp. 1–15, 2022, doi: 10.3390/ani12243452.
- [75] S. Yu et al., “Flavonoids from citrus peel display potential synergistic effects on inhibiting rumen methanogenesis and ammoniogenesis: A microbiome perspective,” *Environmental Science and Pollution Research*, vol. 31, pp. 21208–21223, 2024, doi: 10.1007/s11356-024-32509-5.
- [76] F. Hassan et al., “Phytogenic additives can modulate rumen microbiome to mediate fermentation kinetics and methanogenesis through exploiting diet–microbe interaction,” *Frontiers in Veterinary Science*, vol. 7, p. 575801, 2020, doi: 10.3389/fvets.2020.575801.
- [77] Z. Teng et al., “Tea polyphenols inhibit methanogenesis and improve rumen epithelial transport in dairy cows,” *Animals (Basel)*, vol. 14, no. 17, p. 2569, Sep. 2024, doi: 10.3390/ani14172569.
- [78] T. Tseten, R. A. Sanjorjo, M. Kwon, and S. W. Kim, “Strategies to mitigate enteric methane emissions from ruminant animals,” *Journal of Microbiology and Biotechnology*, vol. 32, no. 3, pp. 269–277, 2022, doi: 10.4014/jmb.2202.02019.